U.S. DEPARTMENT OF THE INTERIOR
U.S. GEOLOGICAL SURVEY

TO ACCOMPANY MAP MF-2378

SEISMIC LANDSLIDE HAZARD FOR THE CITY OF BERKELEY, CALIFORNIA

By Scott B. Miles and David K. Keefer

NONTECHNICAL SUMMARY

This map depicts a possible scenario of hazard due to earthquake-induced landslides within the city of Berkeley, California. The map is intended as a tool for regional planning. Any site-specific planning or analysis should be undertaken with the assistance of a qualified geotechnical engineer. This hazard map should not be used as a substitute to the State of California Seismic Hazard Zones map for the same area (California Department of Conservation, Division of Mines and Geology, 1999). This map should not be used as a basis to determine the absolute risk from seismically triggered landslides at any locality, as the sole justification for zoning or rezoning any parcel, for detailed design of any lifeline, for site-specific hazard-reduction planning, or for setting or modifying insurance rates.

The hazard depicted by this map was modeled for a scenario corresponding to an **M**=7.1 earthquake on the Hayward Fault. This scenario magnitude is associated with complete rupture of the northern and southern segments of the Hayward Fault, an event that has an estimated return period of about 500 years (Working Group on California Earthquake Probabilities, 1999). The modeled hazard also corresponds to completely saturated ground-water conditions resulting from an extreme storm event or series of storm events. (See Miles and Keefer (2000) or Miles and Keefer (1999) for a comparison of the effects of dry and saturated ground-water conditions.) This combination of earthquake and ground-water scenarios represents a particularly severe state of hazard for earthquake-induced landslides. For dry ground-water conditions, the overall hazard will be less, while the relative patterns of hazard are not likely to change.

Levels of hazard depicted by the map should be interpreted on a relative basis. The map includes six levels of relative hazard: *Low*, *Moderately Low*, *Moderate*, *Moderately High*, *High*, and *Very High*. Thus, zones of *High* hazard should be interpreted as having a modeled hazard that is greater than *Moderately High* and less than *Very High*. Whereas, zones of *Low* hazard may be interpreted as having the lowest relative hazard within the mapped area. However, in locations of steep slope or immediate proximity to the Hayward Fault, landslides are possible within zones of *Low* hazard due to mechanisms not modeled by the method described below. For the purposes of interpretation, it may be useful to view the modeled hazard as a concentration (for example, number of landslides per square kilometer). Thus, zones of *Very High* hazard may experience some dense concentrations of landslides, while *Low* hazard zones will only experience a few isolated landslides. Although the likelihood of slope failure increases with greater levels of hazard, the actual area effected by landslides within each given level of hazard will be only a small to moderate percentage of the overall area of the particular hazard zone. Note that most areas of highest hazard are associated with relatively weak bedrock units east of the Hayward Fault.

Areas of slope less than 5 degrees from the horizontal were not analyzed because of negligible hazard from landslides (Keefer, 1984). However, such areas may be susceptible to liquefaction, and a more complete evaluation for the potential for earthquake-induced ground deformation may be obtained by using this map in combination with a map of liquefaction hazard, such as that published by the California Department of Conservation, Division of Mines and Geology (1999).

The map was created using the model of Jibson and others (1998). The model is based on the sliding-block analogy of Newmark (1965), which treats a potential landslide as a rigid block resting on an inclined plane. The model requires inputs characterizing the susceptibility to slope failure and intensity of earthquake ground motion. In essence, the procedure considers the factors of earthquake magnitude, distance to the fault, strength of geologic material, ground water conditions, and hill slope. Susceptibility to slope failure was characterized by treating each 10-meter pixel within the map as an infinitely long slope and estimating the earthquake ground motion required to displace the slope. Earthquake ground motion was characterized using the Arias intensity model of Wilson (1993), together with the selected scenario magnitude (**M**=7.1) and the distance of each pixel from the Hayward Fault. The modeling procedure is described in detail within the technical explanation.

In interpreting any hazard map, it is important to consider the limitations of the model employed and the inherent uncertainties in parameterizing the model. The sliding-block analogy (Newmark, 1965) was developed for analyzing man-made dams and embankments, and, thus, does not consider the mechanisms of failure for soil and rock falls, disrupted soil and rock slides, and liquefaction-induced landslides (see Keefer, 1984, for information on the types of landslides caused by earthquakes). The models of Jibson and others (1998) and Wilson (1993) are well-used alternatives among a number of viable models. Use of different models in the construction of this map may lead to different results, with the relative hazard being similar (see the technical explanation for further information). The uncertainty associated with the model parameters varies with respect to the particular parameter and the level of aggregation (that is, size of support). Due to a lack of earthquake records for the Hayward Fault, the greatest degree of uncertainty is likely associated with the expected levels of earthquake-shaking intensity. The uncertainty associated with the relative strengths between geologic units is smaller. However, the absolute strength within a particular geologic unit is highly variable and, hence, uncertain.

TECHNICAL EXPLANATION

SOCIO-ECONOMIC IMPACT OF EARTHQUAKE-INDUCED LANDSLIDES

Earthquake-triggered landslides have caused huge economic losses and casualties and thus are one of the most damaging collateral effects of earthquakes (Keefer, 1984). One of the most devastating examples is the Nevados Huascarán rock avalanche triggered by the 1970 Peru earthquake (**M**=7.8), which buried two cities and killed about 18,000 people (Plafker and others, 1971). Closer at hand, landslides caused by the 1989 Loma Prieta, California earthquake (**M**=6.9) damaged at least 200 residences, caused at least $30 million in damage, and blocked highways in the epicentral region for several weeks (Keefer, 1998). More recently, the 1994 Northridge, California earthquake (**M**=6.7) triggered more than 11,000 landslides over a 10,000 km^2 area. The landslides blocked roads, severed pipelines, damaged residences, and generated dense dust clouds that triggered an epidemic of valley fever (Harp and Jibson, 1995). Most recently, the Chi-Chi, Taiwan earthquake of 1999 (**M**=7.6) triggered more than 7,200 landslides, which killed at least 49 people and also caused considerable damage.

SEISMIC SLOPE-PERFORMANCE ANALYSIS

Newmark (1965) noted that the transient motions of an earthquake may lead to deformation of a slope prior to complete failure. A Newmark analysis models a potential landslide as a rigid friction-block, having a known critical acceleration, resting on an inclined plane. The analysis calculates the cumulative displacement of the friction-block as it is subjected to the accelerations of a given earthquake time-history. This is done by double-integrating those parts of the earthquake time-history that exceed the critical acceleration (Wilson and Keefer, 1983). Thus, conducting a conventional Newmark analysis requires selection of an appropriate earthquake record and determination of the critical acceleration of the selected slope. Critical acceleration (a_c) can be calculated using the equation developed by Newmark (1965) for the case of planar slip:

$$a_c = (FS - 1)\sin\ \alpha \qquad \textbf{(1)}$$

FS is the static factor of safety of the slope and α is the thrust angle of the landslide block, which is typically approximated by the slope angle.

To avoid the computational complexity and difficulties of selecting an appropriate earthquake time-history associated with a conventional Newmark analysis, several simplified models for estimating Newmark displacements (D_N) have been developed (Luzi and Pergalani, 1999; Jibson and others, 1998; Jibson, 1993; Yegian and others, 1991; Ambraseys and Menu, 1988). One of the most popular simplified Newmark models was developed by Jibson (1993). This relationship is based on Arias intensity (I_a), rather than peak ground acceleration, to better characterize the damaging effects of ground motion. The regression equation was calibrated by double-integrating eleven acceleration time histories, including ten from California, with Arias intensities less than 10 m/s over a range of critical acceleration values (0.02 - 0.40g). The relationship was later updated using 555 records from 13 earthquakes (Jibson and others, 1998). The most current relationship takes the following form:

$$\log D_N = 1.521 \log I_a - 1.993 \log a_c - 1.546 \qquad \textbf{(2)}$$

GIS-BASED NEWMARK'S ANALYSIS

A Newmark analysis can be extended to regional analysis using geographic information systems (GIS). The procedure is summarized by the flow diagram of figure 1, where each labeled box, except for Earthquake Magnitude, represents a map or grid. Conducting a GIS-based Newmark analysis requires creation of a critical acceleration map. This is done by applying Equation 1 to each pixel in the map. The thrust angle for each pixel is approximated by calculating slope from a digital elevation model (DEM). The most common means of calculating the static factor of safety, in the context of spatial analysis, is to apply the infinite slope model to each pixel. Using the infinite slope model, the static factor of safety of a slope (*FS*) can be expressed as follows:

$$FS = \frac{c'}{\gamma d \sin\alpha} + \frac{\tan\phi'}{\tan\alpha} - \frac{m\gamma_w \tan\phi'}{\gamma \tan\alpha} \qquad \textbf{(3)}$$

where c' is the effective cohesion, ϕ' is the effective angle of internal friction, γ is the material unit weight, γ_w is the unit weight of water, α is the angle of the slope from the horizontal, d is the normal depth to the failure surface, and m is the ratio of the height of the water table above the failure surface to d. To apply the infinite slope model using GIS, a map of each parameter is required. Alternatively, a particular parameter can be assumed to be constant throughout the analysis area.

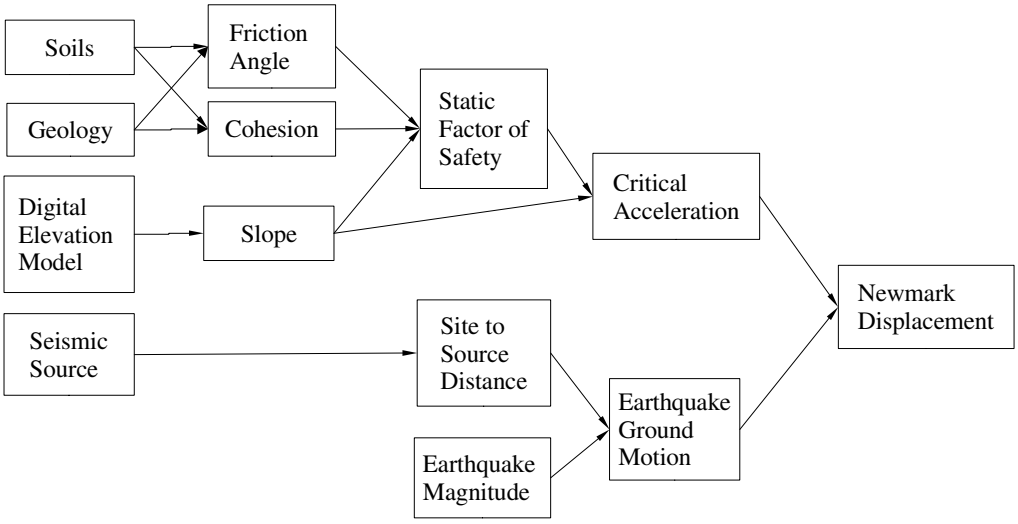

Figure 1. General procedure for conducting a GIS-based Newmark analysis (after Jibson and others, 1998).

Conducting a GIS-based Newmark analysis requires characterization of expected regional earthquake ground motions. The required descriptor of ground motion varies with the specific Newmark model used. In the case of the simplified model of Jibson and others (1998) (Equation 2), the required ground motion descriptor is Arias intensity (I_a). Expected mean Arias intensity can be estimated using the relationship of Wilson (1993).

$$\log I_a = M - 2\log\sqrt{R^2 + h^2} - 4.1 \quad \textbf{(4)}$$

M is moment magnitude, *R* is the minimum horizontal distance, in kilometers, to the vertical projection of the fault rupture surface, and *h* is a depth correction factor that defaults to 7.5 km.

The final step in conducting a GIS-based Newmark analysis is to calculate a map of Newmark displacement based on the maps of critical acceleration and earthquake ground motion. With GIS, it is most convenient to use a simplified Newmark model, such as Jibson and others (1998), to perform this step; however, it is possible to implement the conventional Newmark analysis using the C routine NMGRID (Miles and Keefer, 2000; Miles and Ho, 1999). Calculated Newmark displacement will likely differ for any given locality depending on the particular Newmark model (and, thus, earthquake ground motion model) employed. Hazard maps created using four different GIS-based Newmark models were compared in Miles and Keefer (2000, 1999). Because of the multiplicity of Newmark-based models and their respective output, it is suggested that the results of several models be considered within any decision-making or planning context. The practitioner wishing to incorporate earthquake-induced landslide hazard in such a context should refer to Miles and Keefer (2000) and Miles and others (2000).

CONSTRUCTION OF THE SEISMIC LANDSLIDE HAZARD MAP

This map was created with the simplified Newmark model of Jibson and others (1998) (Equation 2) and the Arias intensity relationship of Wilson (1993) (Equation 4) following the general procedure outlined in the previous section for conducting a GIS-based Newmark analysis (fig. 1). The map represents a scenario **M**=7.1 earthquake — corresponding to complete rupture of the southern and northern segments of the Hayward Fault — and completely saturated ground water conditions.

The data required for calculating static factor of safety and critical acceleration are regional hill slopes and regional geotechnical properties (see Equation 1 and Equation 3). Hill slopes were calculated from a grid of elevation composed of 10-meter (7.5 minute) USGS DEMs derived from contour lines of 1:24,000 quadrangle maps. The steepest calculated slopes in the area analyzed are about 55 degrees from the horizontal.

Regional geotechnical properties were assigned to the geologic units of the 1:24,000 digital geologic map of Graymer and others (1996). The unit weight of geotechnical materials was assumed a constant 20 kN/m^3. Shear strength properties —

effective friction-angle and effective cohesion — were characterized using a three-step process. Each geologic unit within the Graymer and others (1996) geologic map was given a relative rating based on the general slope stability assessments by Radbruch (1969) of units within the 7.5 minute Oakland East, California quadrangle (1:24,000). The ratings used by Radbruch (1969) were *Poor*, *Fair*, *Varies*, and *Good*. Geologic units with ratings of *Poor* and *Good* (the weakest and strongest, respectively) were assigned friction-angle and cohesion values based on the minimum and maximum shear strength values from a database compiled by California Department of Conservation, Division of Mines and Geology (1999). The remaining two ratings were given proportionate values. The final step was to calculate a map of static factor of safety for completely dry conditions (m = 0, Equation 3) to determine if there were any pixels with a factor of safety less than one. In order to apply Equation 3, a constant slope-failure depth of 3.33 m (10 ft) — a representative value (Keefer, 1984) — was assumed. After Jibson and others (1998), the cohesion of all units was uniformly increased until all pixels within the analysis area had a static factor of safety greater than one for dry conditions. The final parameters for the four ratings used in calculating the map for static factor of safety for saturated conditions (m = 1, Equation 3) are given in table 1.

Table 1.

Stability Rating (Radbruch, 1969)	Unit Weight, γ (kN/m^3)	Effective Friction Angle, ϕ' (deg.)	Effective Cohesion, c' (kPa)	Total Strength, τ, at 3m (kPa)
Poor	20	15	30	46
Fair	20	25	40	68
Varies	20	30	55	90
Good	20	35	70	112

The Arias intensity relationship of Wilson (1993) requires three parameters (see Equation 4): moment magnitude, horizontal distance to the vertical projection of the fault plane, and depth-correction factor. A moment magnitude of 7.1 was chosen because it represents complete rupture on the northern and southern segments of the Hayward Fault, which has an estimated return period of 523 years (Working Group on California Earthquake Probabilities, 1999). A depth-correction factor of 10 km was chosen because it provides reasonable estimates of Arias intensities and is consistent with previous application of Wilson (1993) and other similarly based models (Miles and Keefer, 2000; Miles and Ho, 1999). Source-to-site distances were calculated from a digitized trace of the Hayward Fault mapped at a scale of 1:24,000. Calculated Arias intensities range from 10m/s to 13m/s with a mean of 12.3m/s, reflecting the nearness of the Hayward Fault.

Newmark displacements were calculated based on the maps of Arias intensity and critical acceleration using Equation 2. Areas of slope less than 5 degrees were excluded from analysis because of negligible hazard from landslides (Keefer, 1984). Newmark displacements range from 0.7 cm to a truncated maximum of 100 cm (there were a negligible number of pixels with Newmark displacements greater than 100 cm), with a mean of 6.5 cm. To produce the final map depicting relative hazard, the Newmark displacement map was normalized by the maximum value (100 cm) and divided into six categories of relative hazard: *Low* (0 - 0.02), *Moderately Low* (0.02 - 0.05), *Moderate* (0.05 - 0.10), *Moderately High* (0.10 - 0.20), *High* (0.20 - 0.50), and *Very High* (0.50 - 1.00). The results of the GIS-based Newmark analysis are classified in this manner because, for regional analysis, Newmark displacement is considered a relative index of slope-performance, rather than an estimation of real-world deformation (Jibson and others, 1998).

REFERENCES

Ambraseys, N.N. and Menu, J.M., 1988, Earthquake-induced ground displacements: Earthquake Engineering and Structural Dynamics, v. 16, p. 985-1006.

California Department of Conservation, Division of Mines and Geology, 1999, State of California seismic hazard zones: Parts of the Oakland East, Briones Valley, and Las Trampas Ridge Quadrangles, preliminary review map: scale 1:24,000, http://www.consrv.ca.gov/dmg/shezp/maps.htm.

Graymer, R.W., Jones, D.L., and Brabb, E.E., 1996, Preliminary geologic map emphasizing bedrock formations in Alameda County, California: A digital database: U.S. Geological Survey Open-File Report 96-252, http://geology.wr.usgs.gov/open-file/of96-252/.

Harp, E.L., and Jibson, R.W., 1995, Inventory of landslides triggered by the 1994 Northridge, California earthquake: U.S. Geological Survey Open-File Report 95-213, 17 p., http://greenwood.cr.usgs.gov/pub/open-file-reports/ofr-95-0213/.

Jibson, R.W., 1993, Predicting earthquake-induced landslide displacements using Newmark's sliding block analysis: Transportation Research Record 1411, p. 9-17.

Jibson, R.W., Harp, E.L., and Michael, J.A., 1998, A Method for Producing Digital Probabilistic Seismic Landslide Hazard Maps: An Example from the Los Angeles, California area: U.S. Geological Survey Open-File Report 98-113, 17 p., 2 pl., http://geohazards.cr.usgs.gov/pubs/ofr/98-113/ofr98-113.html

Keefer, D.K., 1984, Landslides caused by earthquakes: Geological Society of America Bulletin, v. 95, p. 406-421.

Keefer, D.K., ed., 1998, The Loma Prieta, California, earthquake of October 17, 1989 – landslides: U.S. Geological Survey Professional Paper 1551-C, 183 p.

Luzi, L., and Pergalani, F., 1999, Slope instability in static and dynamic conditions for urban planning: the "Oltre Po Pavese' case history (Regione Lombardia – Italy): Natural Hazards, v. 20, p. 57-82.

Miles, S.B., and Ho, C.L., 1999, Rigorous landslide hazard zonation using Newmark's method and stochastic ground motion simulation: Soil Dynamics and Earthquake Engineering, v. 18, no. 4, p. 305-323.

Miles, S.B., and Keefer, D.K., 1999, Comparison of seismic slope-performance models: case study of the Oakland East Quadrangle, California: U.S. Geological Survey Open-File Report 99-137, http://salish.wr.usgs.gov/pubs/ofr-99-137/.

Miles, S.B., and Keefer, D.K., 2000, Evaluation of seismic slope-performance models using a regional case study: Environmental & Engineering Geoscience, v. 11, no. 1 p. 25-39.

Miles, S.B., Keefer, D.K., and Nyerges, T.L., 2000, A case study in GIS-based environmental model validation using earthquake-induced landslide hazard, *in* Heuvelink, G. B. M., and Lemmens, M. J. P. M., eds., 4th International Symposium on Spatial Accuracy Assessment in Natural Resources and Environmental Sciences: Amsterdam, Delft University Press, p. 481-493.

Newmark, N.M., 1965, Effects of earthquakes on dams and embankments: Geotechnique, v. 15, p. 139-160.

Plafker, George, Ericksen, G.E., and Concha, J.F., 1971, Geological aspects of the May 31, 1970, Perú Earthquake: Bulletin of the Seismological Society of America, v. 61, p. 543-587.

Radbruch, D.H., 1969, Areal engineering geology of the Oakland East quadrangle: U.S. Geological Survey Map GQ-769.

Wilson, R.C., 1993, Relation of Arias intensity to magnitude and distance in California: U.S. Geological Open-File Report 93-556, 41 p.

Wilson, R.C., and Keefer, D.K., 1983, Dynamic analysis of a slope failure from the 6 August, 1979 Coyote Lake, California, earthquake: Seismological Society of America Bulletin, v. 73, no. 3, p. 863-877.

Working Group on California Earthquake Probabilities, 1999, Earthquake probabilities in the San Francisco Bay Region: 2000 to 2030 - A summary of findings: U.S. Geological Survey Open-File Report 99-517, http://geopubs.wr.usgs.gov/open-file/of99-517/.

Yegian, M.K., Marciano, E., and Ghahraman, V.G., 1991, Earthquake-induced permanent deformations: probabilistic approach: Journal of Geotechnical Engineering, ASCE, v. 17, no. 1, p. 35-50.

readme.txt

Contents of berkdb.zip

dn-plot.e00	Arc/Info exchange file of hazard values GRID
berkbound.e00	Coverage containing Berkeley city boundary
berkhayward.e00	Coverage containing portion of Hayward fault w/in Berkeley limits
berkmajrds.e00	Coverage containing major roads w/in Berkeley limits
berkmajint.e00	Coverage containing major intersections w/in Berkeley limits
berkstreets.e00	Coverage containing streets w/in Berkeley limits
coast.e00	Coverage containing arcs and polygons used to define coastline

Contents of berkpdf.zip

berkpamph.pdf	PDF of map pamphlet
berkmap.pdf	PDF of hazard map: 36" x 48"

PDFs were generated using GNU Ghostscript. These documents are compatible with Adobe Acrobat 4.0 and versions higher.

Contents of berkeps.zip

berkpamph.pdf	PDF of map pamphlet
berkmap.eps	Encapsulated PostScript plot file of hazard map: 36" x 48"

Fonts are embedded, there are no thumbnails or previews.

For questions related to files enclosed in these data packages, contact Scott Miles at 650-329-4820 or smiles@usgs.gov